Kovove Mater. 59 2021 187–194
DOI: 10.4149/km_2021_3_187

Effect of mill scale usage on thermodynamic modeling and metallothermic production of FeMn alloys

M. Bugdayci

Yalova University, Chemical Engineering Department, Yalova, 77200, Turkey

Received 1 May 2021, received in revised form 1 June 2021, accepted 6 June 2021

Abstract

Ferromanganese (FeMn) is an alloy that is generally used to increase the wear resistance of steels and can be produced with high energy systems. In this study, the material produced by the metallothermic reduction method and a serious energy saving is achieved. In studies conducted for FeMn production, optimum recovery conditions were determined for varying aluminum stoichiometries. In addition, mill scale was used as a source to obtain the Fe structure in the alloy, and waste material was evaluated. In addition, magnetite was used as a source of iron oxide, and the recovery values of these products were compared with the mill scale. The characterization of the produced materials was determined by XRD, optical microscope and hardness methods. According to the results, the highest recovery is 110 % Al stoc. with magnetite, 98.58 % for Fe, and 85 % for Mn. The hardness value of the same sample gave the highest result with 64.65 HRC.

K e y w o r d s: FeMn, mill scale, recycling, metallothermic reduction, combustion synthesis, thermodynamic modeling

1. Introduction

The decrease of natural resources in the world has made the use of waste a very important issue. Material consumption is increasing day by day with the effect of new technologies and more material requirements. At this point, recycling and production from secondary sources are of great importance. This situation both saves primary resources and provides less energy consumption [1–4].

In the production of ferromanganese from primary sources, a large amount of waste is generated in the settling tanks that store the wastewater in the facilities; they originate predominantly from raw material storages (e.g., manganese ore and reducing agents), drainage gutters and slag. This waste amount has been determined as approximately 50 kg per ton of alloy [3, 5–7].

Manganese is an important metal that finds a wide range of use. This material is evaluated in a wide spectrum from the food industry to the production of nonferrous compounds, arsenic absorption battery applications and ferroalloy production [8–11].

Ferromanganese (FeMn), one of the iron-based alloys, is traditionally produced by the casting method. The storage of flue gases poses an important problem in this process, given environmental concerns. In addition, in iron alloy casting containing Mn, when the Mn amount in the charge exceeds 20 %, the melt turns into a very viscous structure. The casting of the material is very difficult due to the difficulty in metal flow. In addition, the solidification phase of the material cast in the mold is also quite problematic, because the increase in the amount of Mn in the melt increases the viscosity of the liquid. Since sufficient fluidity cannot be obtained from the metal, the mold should deteriorate rapidly, and the sample should be cooled quickly [12, 13].

Considering all these problems, adding Mn to the liquid iron bath as FeMn makes the process much easier, because the material will be of similar density in the liquid phase of the steel and the desired composition will be obtained easily. Casting without increasing viscosity will prevent the problems mentioned above [14–16].

Mill scale is a precious waste containing approxi-

*Corresponding author: e-mail address: mehmet.bugdayci@yalova.edu.tr

Table 1. Chemical composition of mill scale (%)

Material	Fe°	Fe^{+2}	Fe^{+3}	Mn	Cu	Total Fe
Mill Scale	3.56	24.59	42.80	0.75	0.14	70.95

	Fe	Cr	Ni	Zn	Mn	Mg	Al	Mo	Si
Al	0.028	0.29	0.004	0.56	0.45	4.65	Bal.	Trace	0.12

mately 70 % Fe-based structure, which is formed during the annealing of steel plates and billets and during the cooling of the steel structure in continuous casting plants [17–19].

Since mill scale is formed in very high amounts in the processes mentioned above, its recycling is important. This material is currently used as an additive in many applications. One of the most common uses is to add it to portland cement. Mill scale is also used for lead removal from aqueous solutions and electromagnetic shielding applications [20–23].

FeMn casting alloys have a Mn content from 17 to 28 % [12, 24]. In the study of Florez et al., the corrosion behavior of high manganese steels was examined, and chemical compositions of 20 Mn, 22 Mn, 26 Mn, and 28 Mn FeMn alloys were determined. Accordingly, 22 Mn alloy consists of 22.22 % Mn, 3.39 % Al, and the rest is Fe. This compound was chosen as the target composition in this study [24].

In this study, it is aimed to optimize FeMn production parameters by using metallothermic method with reference to different iron oxide sources. The effects of varying Al stoichiometries on recoveries, microstructures and mechanical properties were determined.

2. Material

Magnetite (Fe_3O_4) and mill scale (Fe + FeO + Fe_2O_3) were used as iron sources in experimental studies. Oxidized manganese was used as the source of Mn, while aluminum was reacted as a reductant. The properties of the materials used are given in Table 1. The chemical compositions of the materials were determined by atomic absorption spectrometry (AAS, Perkin Elmer Analyst 800) techniques.

In addition to the materials used in Table 1, Merck 60 mesh 99 % purity MnO was used as a source of Mn.

The realization of the process in the metallothermic process depends on thermodynamic principles. The first of the principles mentioned is the Gibbs free energy (ΔG) balance. Gibbs free energy values can be observed by looking at the Ellingham diagram of the oxides. In this diagram, the metallic material with a more negative ΔG value is capable of reducing the oxidized structure without requiring any additional energy [25]. Accordingly, the materials below in the

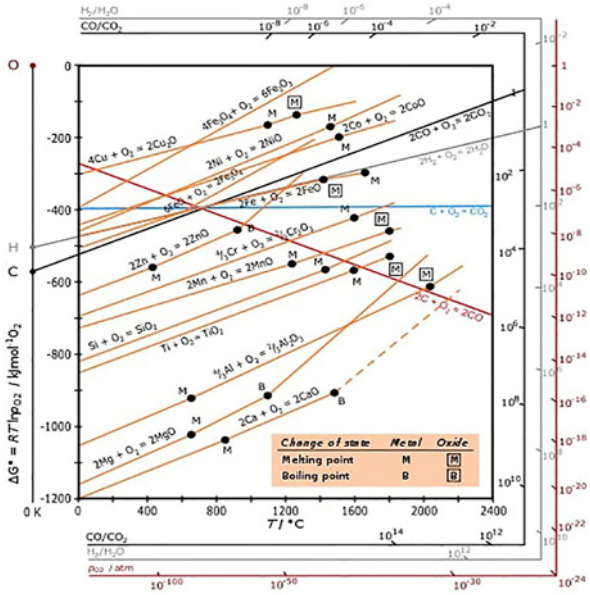

Fig. 1. Oxides Ellingham diagram [26].

diagram can reduce the above. Figure 1 shows the Ellingham diagram of the oxides. According to the figure, MnO and FeO structures are above the aluminum in the diagram. The reduction of manganese oxide is indicated by a blue arrow, while that of iron oxide is indicated by a brown arrow. Therefore, Al is in a position to reduce these structures easily. The reduction behavior of C is shown in the section marked with blue and red in the graphic. Accordingly, with increasing temperature, CO_2 transforms into CO structure in accordance with the Boduard reaction and can only exhibit behavior that can reduce manganese oxide at a temperature above 1300 ℃. The spontaneous realization of the process in the metallothermic process makes the metallothermic method more advantageous in terms of energy and time compared to the carbothermic reduction method.

Another important parameter in metallothermic applications is the adiabatic temperature (T_{ad}). This value must be at least 1527 ℃; otherwise, the reaction cannot start and proceed by itself. Finally, the specific heat value of the reaction needs to be determined. This value is determined by dividing the reaction enthalpy by the molar weight of the products. Specific

heat value should be higher than 2250 J g^{-1} K^{-1} and lower than 4500 J g^{-1} K^{-1}. If the specific heat is lower than 2250 J g^{-1} K^{-1}, metal slag separation will not occur, whereas if it is higher than 4500 J g^{-1} K^{-1}, high scattering rates will be obtained due to the excessive explosive effect, and the efficiency will decrease. The specific heat and T_{ad} values of the reactions in this study were calculated with the FactSage 7.1. database, and the findings are shown in the Results and discussion section.

While designing the experiments, the amount of aluminum that can reduce the oxidized raw materials was determined as 100 % stoichiometric ratio, then the optimum reduction conditions were determined by changing the Al stoichiometry to be 105, 110, and 115 %. The stoichiometric mixtures in the experiments carried out with mill scale were determined according to Eqs. (1)–(4). The mixtures were prepared so that the total weight of the charge was 50 g:

$$\mathrm{Fe} \rightarrow \mathrm{Fe}, \tag{1}$$

$$\mathrm{Fe_2O_3} + 2\mathrm{Al} \rightarrow 2\mathrm{Fe} + \mathrm{Al_2O_3}, \tag{2}$$

$$3\mathrm{FeO} + 2\mathrm{Al} \rightarrow 3\mathrm{Fe} + \mathrm{Al_2O_3}, \tag{3}$$

$$3\mathrm{MnO} + 2\mathrm{Al} \rightarrow 3\mathrm{Mn} + \mathrm{Al_2O_3}. \tag{4}$$

The same study was carried out for magnetite, and Al stoichiometry was calculated according to Eqs. (4) and (5):

$$3\mathrm{Fe_3O_4} + 8\mathrm{Al} \rightarrow 9\mathrm{Fe} + 4\mathrm{Al_2O_3}. \tag{5}$$

The samples were weighed with the stoichiometries determined in the reduction experiments, then processed in a turbula mixer for 30 min, and homogenization of the charge was achieved. The samples removed from the mixer were kept in ETUV at 105 °C for 1 h to be dehumidified. The samples extracted from ETUV were charged to the copper crucible, and the powders were brought to a more solid structure by compacting with an apparatus from the top. Afterwards, Cr-Ni resistance wire was placed on the mixture, and the reaction was triggered by passing current over this wire connected to variac with copper cables. The mixture, which generates its own energy without the need for any extra energy after it is triggered, created a combustion wave from above and performed the reduction process throughout the structure. The flowchart of the process is shown in Fig. 2.

After the metallothermic process was completed, the chemical composition of the metallic samples was determined using the metal mode with the Thermoscientific XRF device. The slag was examined with the soil mode of the same device, as well as X-Ray diffractometer (PANalytical PW3040/60, Cu Kα radiation) equipment with X'Pert High Score databases.

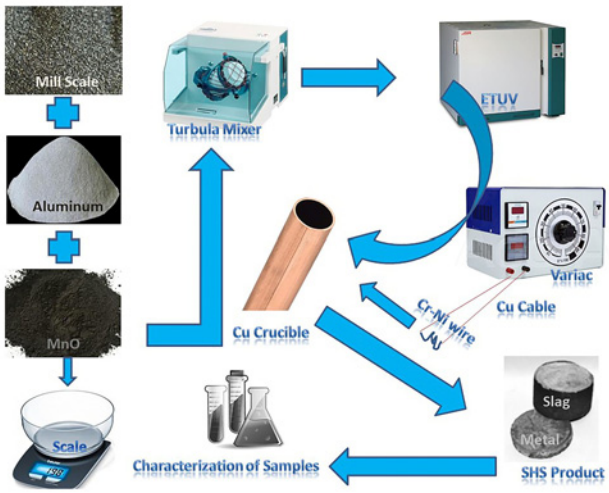

Fig. 2. Flowchart of metallothermic process.

3. Results and discussion

3.1. Thermodynamic calculations

Before starting experimental studies, reduction systems were examined thermodynamically, modeling studies were carried out with the FactSage 7.1 database. In modeling studies, firstly, enthalpy values were calculated by using the reaction module of the program. Based on these values, specific heat (*SH*) values were determined according to Eq. (6):

$$\text{Specific heat} = \frac{\Delta H}{\sum \text{Weight of products}}. \tag{6}$$

Accordingly, the enthalpy and specific heat values of the Fe_2O_3-MnO-Al and Fe_3O_4-MnO-Al reduction systems were calculated via the FactSage reaction module and findings are presented in Eqs. (7) and (8), respectively:

$$\mathrm{Fe_2O_3} + 2\mathrm{MnO} + 3.33\mathrm{Al} \rightarrow 2\mathrm{FeMn} + 1.66\mathrm{Al_2O_3}\Delta H_{298} = -1197190.4\,\mathrm{J},\quad SH = 3109\,\mathrm{J\,g^{-1}\,K^{-1}}, \tag{7}$$

$$\mathrm{Fe_3O_4} + 3\mathrm{MnO} + 4.66\mathrm{Al} \rightarrow 3\mathrm{FeMn} + 2.33\mathrm{Al_2O_3}\Delta H_{298} = -1637780.2\,\mathrm{J},\quad SH = 2873\,\mathrm{J\,g^{-1}\,K^{-1}}. \tag{8}$$

According to Eqs. (7) and (8), it has been determined that the specific heat values are in the range of 2250–4500 J g^{-1} K^{-1}; therefore, it has been understood that metal slag separation can be achieved with the metallothermic process, and production can be made with this method.

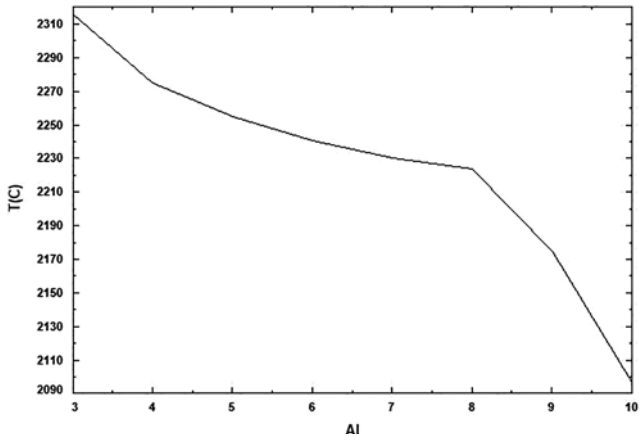

Fig. 3. The adiabatic temperature of Fe_2O_3-MnO system for increased Al.

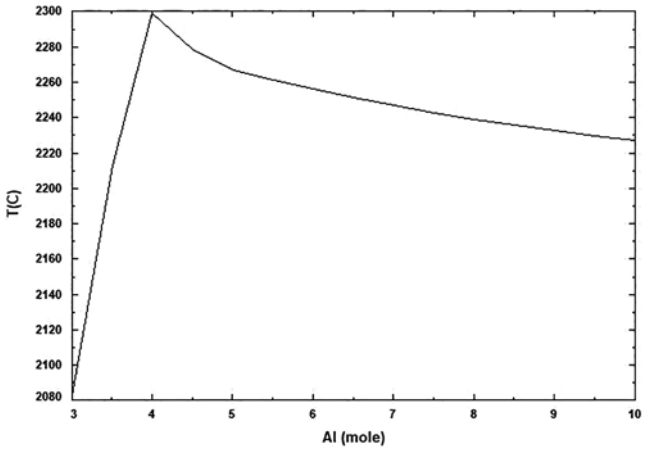

Fig. 4. The adiabatic temperature of Fe_3O_4-MnO system for increased Al.

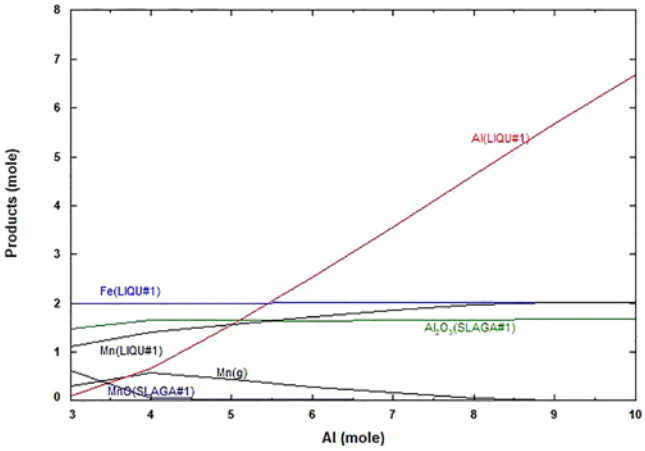

Fig. 5. Probable phases of Fe_2O_3-MnO system for increased Al.

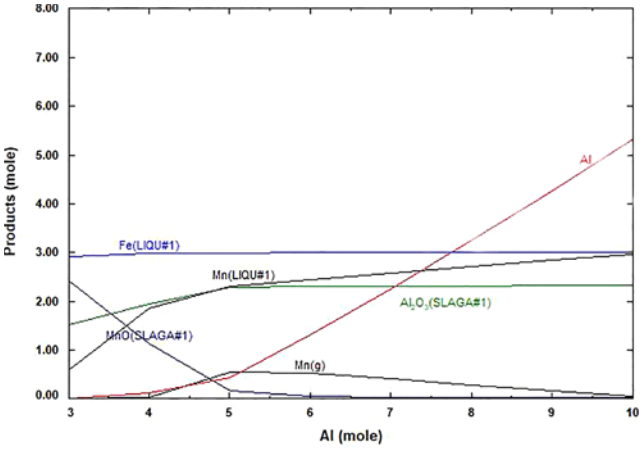

Fig. 6. Probable phases of Fe_3O_4-MnO system for increased Al.

After determining the specific heat values of the reduction systems, the effect of the increasing Al amount on T_{ad} was investigated by using the Equilibrium module of the FactSage 7.1 program. T_{ad} change of Fe_2O_3--MnO-Al reduction system is shown in Fig. 3, while that of Fe_3O_4-MnO-Al is shown in Fig. 4.

When Fig. 3 is examined, it is seen that the adiabatic temperature of the system has increased to 2315 ℃ with the addition of 3 moles of Al. It was determined that this value decreases to 2090 ℃ in 10 moles in the next Al additions. The reason for this is that after the amount of Al exceeds 3 moles, it tries to reduce the Al_2O_3 structure formed in the slag phase. In order to start the process in metallothermic reactions, the T_{ad} value is expected to be at least 1527 ℃. This value is exceeded both in the Fe_2O_3-MnO-Al system in Fig. 3 and in the Fe_3O_4-MnO-Al system in Fig. 4. Therefore, the targeted FeMn composition can be produced by this method.

According to Fig. 4, the highest T_{ad} value (2300 ℃) was reached with the addition of 4 moles of Al. A similar situation seen in Fig. 3 is encountered here as well. However, T_{ad} value of 2240 ℃ was reached with the addition of 10 moles of Al.

The thermodynamic simulation studies of the reduction systems continued with the research of determining the probable phases that occur with the increasing amount of aluminum. In the calculations made with the equilibrium module of the FactSage program, the probable phases expected to be formed from Fe_2O_3-MnO reactants are given in Fig. 5, while the Fe_3O_4-MnO system is examined in Fig. 6.

When Fig. 5 is examined, it is determined that the Fe phase was formed stably at every Al ratio, and the amount of metallic Mn formation increases from 1 mole to 2 moles with increasing Al amount. However, the amount of metallic Al that increases exponentially is observed in Al amounts of more than 3 moles. There-

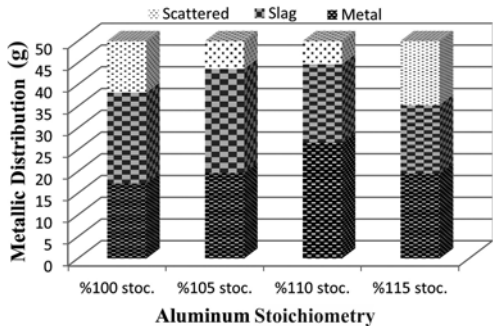

Fig. 7. Mill scale exp. metallic distribution of products for different Al stoichiometries.

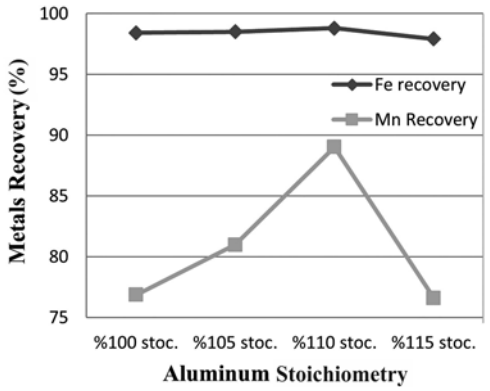

Fig. 8. Mill scale exp. metallic recoveries of products for different Al stoichiometries.

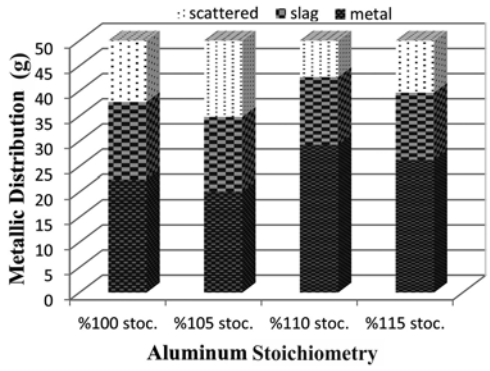

Fig. 9. Magnetite exp. metallic distribution of products for different Al stoichiometries.

fore, the amount of Al required for reduction is determined as calculated in Eq. (7).

Figure 6 shows the possible phases under reduction conditions using magnetite as the iron source. In the graph drawn according to the increasing amount of aluminum, it was seen that Fe can be obtained in a constant manner at every mole ratio as in Fig. 5, and it was determined that the amount of formation decreased after Mn was formed by increasing the amount of Al up to 5 moles.

3.2. Experimental results

In experimental studies, the optimum experimental conditions were determined by reducing the iron-oxide/manganese-oxide structures with metallic aluminum in varying stoichiometric ratios. Mill scale and magnetite were used as iron sources, and their effects on reaction recoveries were investigated. The recoveries of products were calculated according to Eq. (9):

$$\text{Metallic yield} = \frac{\text{The weight of metal after metallothermic reduction}}{\text{The weight of aspect metal after metallothermic reduction}}. \quad (9)$$

The first experimental set was built using mill scale; the Al stoichiometry increased from 100 to 115 % with changes of 5 %. While the metal, slag and scattered values obtained as a result of the experiments are shown in Fig. 7, the metal recovery values are presented in Fig. 8.

According to Fig. 7, the amount of metal formation increased up to 110 % stoichiometric rate and decreased when it reached 115 %. The scattered rate was also observed at the lowest 110 % stoichiometric rate. Accordingly, the amount of Al that can recover the highest amount of metal in the charge obtained from the mixture of mill scale-MnO and Al was determined as 110 % Al stoichiometry. Consistent with the possible phases observed in thermodynamic studies, Fe was obtained with an efficiency over 98 % at each Al ratio. When we look at the amount of Mn recovery, parallel to the metal formation amount, it increased up to 110 % Al stoichiometry (89 %) and decreased by 115 % (76 %). Therefore, experiments were not continued after 115 % stoichiometric rate. The reason for the decrease here is that aluminum, which is formed in the Al ratios after the 110 % Al amount, exhibits behavior in a direction that decreases the total reaction energy by reducing Al_2O_3. The change in adiabatic temperatures observed in Figs. 3 and 4 is consistent with these results.

In the second stage of the experiments, magnetite was used instead of mill scale as the iron source, and the experiments were carried out under the same conditions as the first set. While the metal amounts formed in the experiments performed with magnetite are shown in Fig. 9, the metal recoveries amounts are shown in Fig. 10.

When the experiments conducted with magnetite encountered the results obtained with mill scale, it was seen that the stoichiometry change had exactly the same effect, but the amount of metal obtained in magnetite was higher. In Fig. 9, while 29.27 g of

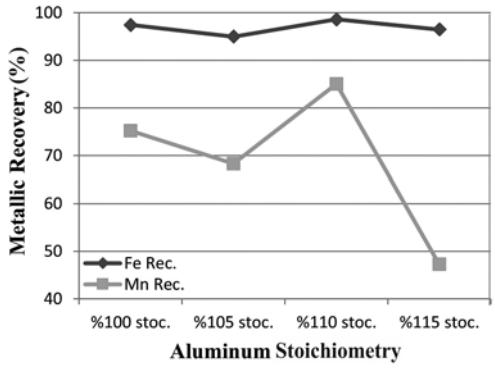

Fig. 10. Magnetite exp. metallic recoveries of products for different Al stoichiometries.

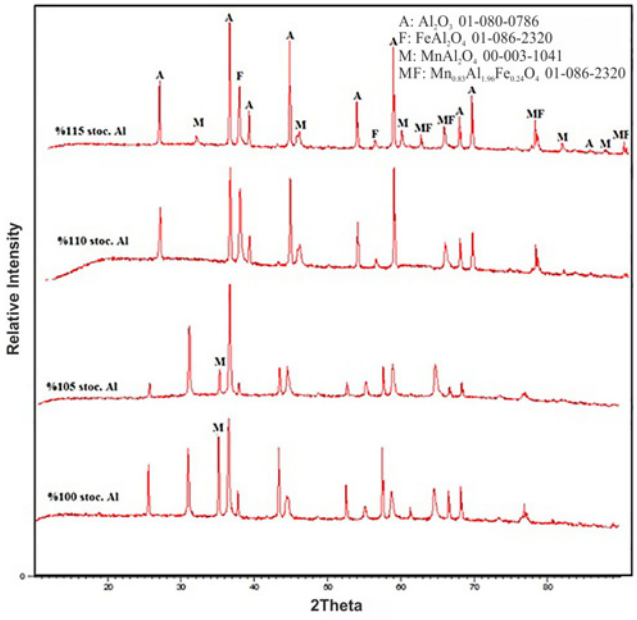

Fig. 11. XRD Results of magnetite based products slags. (*MF phase PDF number: 00-012-0431*).

metal was obtained in 110 % stoichiometric mixture, this value was determined as 26.67 g in the case of mill scale (Fig. 7). When Fig. 10 is examined, it is seen that the change in stoichiometric ratio in the recovery of metallic material behaves similarly to the experiments performed with mill scale. However, when the Mn recoveries in 110 % stoichiometric mixture were compared, an efficiency of 89.02 % was obtained in the set performed with mill scale, while this value was found as 85 % in the magnetite set. Accordingly, it was determined that while the use of magnetite gives the best result in terms of the amount of metal formed, the use of scale for Mn recovery gives the optimum result.

The slags of the experiments carried out with magnetite were also examined with the XRD technique

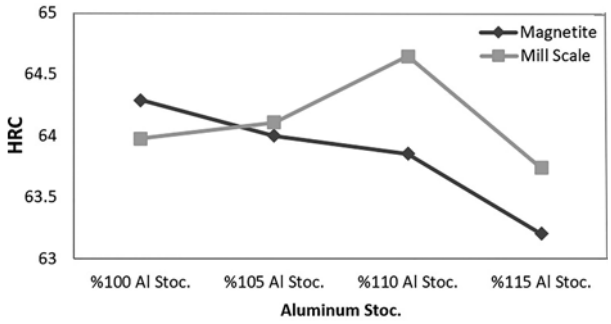

Fig. 12. HRC hardness values of samples.

and the findings are presented in Fig. 11. According to the XRD patterns, it is clearly seen that the main phase formed in the slag was in the structure of Al_2O_3, indicated by A. In all compositions, the highest peak intensity was observed in composition A. In addition to the Al_2O_3 phases, the samples also contain $FeAl_2O_4$ encoded with F, $MnAl_2O_4$ marked with M and $Mn_{0.83}Al_{1.96}Fe_{0.24}O_4$, indicated by MF. It is seen that the M structure formed at 35° in the XRD pattern of mixtures containing 100 and 105 % stoichiometric Al was not seen in later proportions, as well as the intensity of other F, M and MF structures decreased significantly. When the mixtures with 110 and 115 % stoichiometric ratio of XRD peaks were compared, it was determined that M and MF structures, which were seen intensively between 55° and 70° , were seen at 115 % stoichiometric rate, but not at 110 % stoichiometric rate. According to Fig. 9, the mixture with the lowest slag phase is seen as 110 % Al stoichiometry. In the XRD pattern, the M and MF phases did not pass into the slag and remain in the metal, which is consistent with the results in Fig. 9. When Fig. 10 was examined regarding the subject, it was seen that when the amount of metallic manganese changes from 105 to 110 %, it increases from 68 to 85 % in the produced metallic structure; therefore the Mn-based structure that passes to the slag phase decreases. In the XRD analysis made at a stoichiometric rate of 110 %, the decrease in the amount of peaks consisting of M and MF explains the situation in Fig. 10.

After determining the metallic recovery values of the samples, the characterization studies continued with hardness tests. HRC hardness values of the samples are given in Fig. 12. Figure 12 shows that it was determined that the highest hardness value was seen in the sample obtained in 110 % stoichiometric Al mixture experiment. It was determined that this value with the highest recovery of manganese increased the hardness of the material in parallel with the increase in the amount of Mn formed in the structure. When the hardness values of steels containing manganese are examined, it is seen that the hardness of these steels is

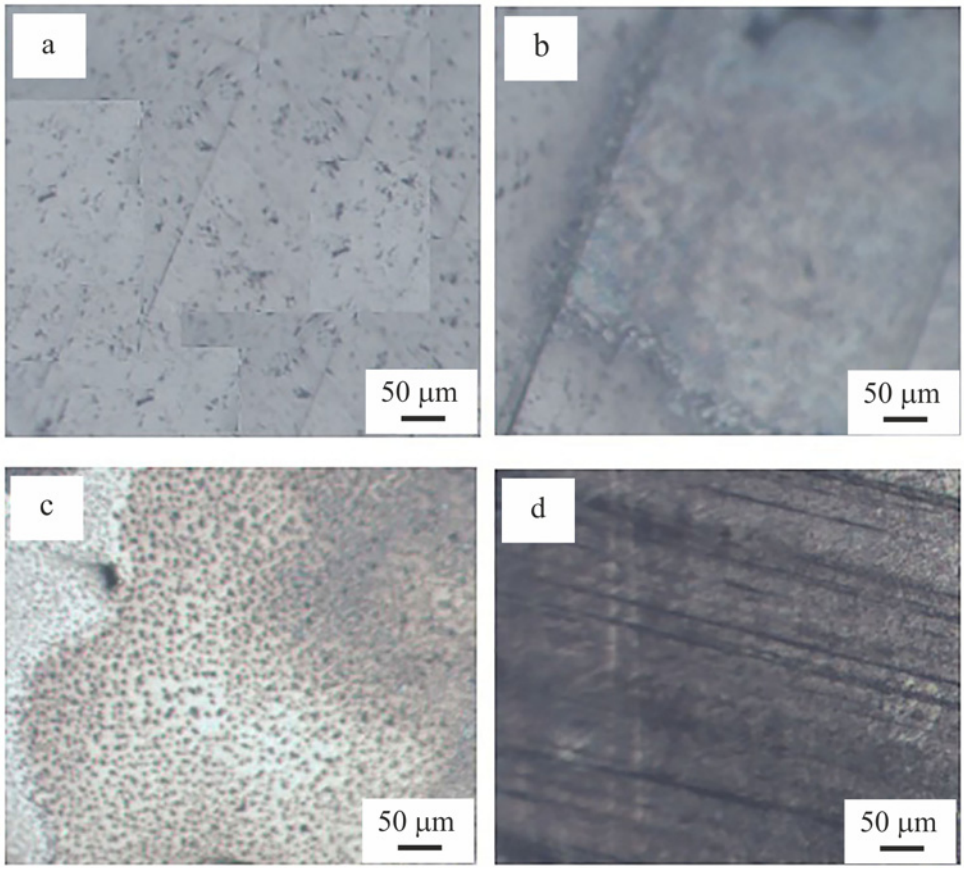

Fig. 13. Optical microscopy results of the samples: (a) 100 % Al stoc., (b) 105 % Al stoc., (c) 110 % Al stoc., and (d) 115 % Al stoc.

in the range of 220 HB to 550 HB [27]. In experimental studies, the hardness of the sample in 110 % stoichiometric mixture corresponds to 711 HB. Accordingly, it has been determined that a higher strength can be achieved with this method for these materials operating in an abrasive environment where the hardness value is important.

In the characterization studies, the macrostructures of the samples were examined by the optical microscopy method. In optical microscopy studies, after the samples were cut and sanded, they were etched with a solution containing 50% HF-50% pure water by volume for 15 min, after which the examinations were carried out. The optical examination was made for the mixtures prepared using a scale, and the findings are shown in Fig. 13.

The optical structure seen in Fig. 13a shows that small Mn and Al-based structures were formed, which appear dispersed in the Fe matrix at 100 % stoichiometric composition. In Fig. 13b, it was determined that these structures are collected and seen more clearly on the matrix. In Fig. 13c, it was determined that the manganese-based intermetallic structure was formed more clearly by forming homogeneous precipitates in the darker region. Accordingly, as seen in Fig. 8, these precipitates increased the Mn recovery, and, as can be understood from Fig. 12, the hardness of the sample increased to the maximum level. In Fig. 13d, it is seen that these precipitations could not occur, and the intermetallic structure made the alloy formation difficult by covering the matrix.

4. Conclusions

This study is aimed to produce cast steel alloys containing Mn by the metallothermic method. Before experimental studies, reduction systems were modeled with FactSage 7.1 program, and optimum production conditions were simulated. In experimental studies based on thermodynamic studies, magnetite and mill scale were used as iron sources. In this way, the mill scale generated as production waste was recycled. In experimental studies, manganese was reduced from oxidized Mn structures, and Al powder was used as a reductant. Al stoichiometry was changed from 100 to 115 % with 5 % differences in the experiments, and the findings were interpreted through the recoveries. After the experimental studies were completed, the products were characterized, and the highest recovery

was observed in 98.58 % Fe, 85 % Mn values and 110 % stoichiometric magnetite mixture. The samples were also examined by XRD and optical microscope methods and the best results were observed in the same sample as well as in recoveries. The hardness values of the samples were also determined according to the HRC scale, the hardest sample was determined in a 110 % stoichiometric magnetite mixture with a value of 64.65 HRC.

References

[1] S. Yeşiltepe, M. K. Şeşen, Production of composite pellets from waste coffee grounds, mill scale and waste primary battery to produce ferromanganese; a zero waste approach, Acta Metall. Slovaca 26 (2020) 45–48. doi:10.36547/ams.26.2.540

[2] S. Yeşiltepe, M. Buğdaycı, O. Yücel, M. K. Şeşen, Recycling of alkaline batteries via a carbothermal reduction process, Batteries 5 (2019) 35. doi:10.3390/batteries5010035

[3] T. G. Cota, E. L. Reis, R. M. F. Lima, R. A. S. Cipriano, Incorporation of waste from ferromanganese alloy manufacture and soapstone powder in red ceramic production, Appl. Clay Sci. 161 (2018) 274–281. doi:10.1016/j.clay.2018.04.034

[4] I. M. C. Lo, X. Y. Yang, Removal and redistribution of metals from contaminated soils by a sequential extraction method, Waste Manag. 18 (1998) 1–7. doi:10.1016/S0956-053X(97)10005-8

[5] A. Mladenović, J. Turk, J. Kovač, A. Mauko, Z. Cotić, Environmental evaluation of two scenarios for the selection of materials for asphalt wearing courses, J. Clean. Prod. 87 (2015) 683–691. doi:10.1016/j.jclepro.2014.09.013

[6] H. Shen, E. Forssberg, An overview of recovery of metals from slags, Waste Manag. 23 (2003) 933–949. doi:10.1016/S0956-053X(02)00164-2

[7] J. Guo, Y. Bao, M. Wang, Steel slag in China: Treatment, recycling, and management, Waste Manag. 78 (2018) 318–330. doi:10.1016/j.wasman.2018.04.045

[8] B. Ghafarizadeh, F. Rashchi, E. Vahidi, Recovery of manganese from electric arc furnace dust of ferromanganese production units by reductive leaching, Miner. Eng. 24 (2011) 174–176. doi:10.1016/j.mineng.2010.11.003

[9] F. Ferella, I. De Michelis, F. Beolchini, V. Innocenzi, F. Vegliò, Extraction of zinc and manganese from alkaline and zinc-carbon spent batteries by citric-sulphuric acid solution, Int. J. Chem. Eng. 2010 (2010) 659434. doi:10.1155/2010/659434

[10] E. Sayilgan, T. Kukrer, N. O. Yigit, G. Civelekoglu, M. Kitis, Acidic leaching and precipitation of zinc and manganese from spent battery powders using various reductants, J. Hazard. Mater. 173 (2010) 137–143. doi:10.1016/j.jhazmat.2009.08.063

[11] N. Jain, A. Maiti, Arsenic adsorbent derived from the ferromanganese slag, Environ. Sci. Pollut. Res. 28 (2021) 3230–3242. doi:10.1007/s11356-020-10745-9

[12] O. E. Falodun, S. R. Oke, A. M. Okoro, P. A. Olubambi, Characterization of cast manganese steels containing varying manganese and chromium additions, Mater. Today Proc. 28 (2019) 730–733. doi:10.1016/j.matpr.2019.12.288

[13] A. D. Subhi, O. A. Abdulrazaq, Phase transformations of Hadfield manganese steels, Eng. & Technol. 25 (2007) 808–811.

[14] L. Öncel, Production of ferronickel from mill-scale via metallothermic process, El-Cezeri J. Sci. Eng. 7 (2020) 824–834. doi:10.31202/ecjse.702804

[15] L. Öncel, Production of ferromolybdenum from mill scale via aluminothermic process, Sinop Uni. J. Nat. Sci. (2020) 64–76. doi:10.33484/sinopfbd.724720

[16] M. Bugdayci, M. Alkan, A. Turan, O. Yücel, Production of iron based alloys from mill scale through metallothermic reduction, High Temp. Mater. Process. 37 (2018) 889–898. doi:10.1515/htmp-2017-0073

[17] S. Cho, J. Lee, Metal recovery from stainless steel mill scale by microwave heating, Met. Mater. Int. 14 (2008) 193–196. doi:10.3365/met.mat.2008.04.193

[18] M. I. Martín, F. A. López, J. M. Torralba, Production of sponge iron powder by reduction of rolling mill scale, Ironmak. Steelmak. 39 (2012) 155–162. doi:10.1179/1743281211Y.0000000078

[19] J. W. Park, J. C. Ahn, H. Song, K. Park, H. Shin, J. S. Ahn, Reduction characteristics of oily hot rolling mill sludge by direct reduced iron method, Resour. Conserv. Recycl. 34 (2002) 129–140. doi:10.1016/S0921-3449(01)00098-2

[20] G. Bantsis, C. Sikalidis, M. Betsiou, T. Yioultsis, T. Xenos, Electromagnetic absorption, reflection and interference shielding in X-band frequency range of low cost ceramic building bricks and sandwich type ceramic tiles using mill scale waste as an admixture, Ceram. Int. 37 (2011) 3535–3545. doi:10.1016/j.ceramint.2011.06.010

[21] Y. I. Murthy, Stabilization of expansive soil using mill scale, Int. J. Eng. Sci. Technol. 4 (2012) 629–632.

[22] Y. Rajshekar, J. Pal, T. Venugopalan, Mill scale as a potential additive to improve the quality of hematite ore pellet, Miner. Process. Extr. Metall. Rev. 39 (2018) 202–210. doi:10.1080/08827508.2017.1415205

[23] O. Yucel, F. Demirci, A. Turan, M. Alkan, Determination of direct reduction conditions of mill scale, High Temp. Mater. Process. 32 (2013) 405–412. doi:10.1515/htmp-2012-0167

[24] M. A. Cerra Florez, M. N. Da Silva Lima, W. S. Araújo, M. J. G. Da Silva, Characterization and comparative analysis of corrosion resistance of 4 high manganese steels models in aqueous solution of NaCl, Mater. Res. 22 (2019) 1–13. doi:10.1590/1980-5373-MR-2019-0283

[25] M. Bugdayci, G. Deniz, C. Ziyreker, A. Turan, L. Oncel, Thermodynamic modeling and production of FeCo alloy from mill scale through metallothermic reduction, Eng. Sci. Technol., an Int. J. 23 (2020) 1259–1265. doi:10.1016/j.jestch.2020.03.003

[26] M. Buğdayci, A. Turan, Metallothermic production of FeCo and FeCoV alloys and the thermodynamical modeling studies of the process, BEU Journal of Science 9 (2020) 264–276. (in Turkish)

[27] https://titussteel.com/our-products/wear-and-impact-steel/titus-manganese/ date of access: 04/30/2021